

Reports

Missile Impacts as Sources of Seismic Energy on the Moon

Abstract. *Seismic signals recorded from impacts of missiles at the White Sands Missile Range are radically different from the signal recorded from the Apollo 12 lunar module impact. This implies that lunar structure to depths of at least 10 to 20 kilometers is quite different from the typical structure of the earth's crust. Results obtained from this study can be used to predict seismic wave amplitudes from future man-made lunar impacts. Seismic energy and crater dimensions from impacts are compared with measurements from chemical explosions.*

The Apollo passive seismic experiment team has recently reported first results from the impact of the ascent stage of the lunar module (LM) on the lunar surface as part of the Apollo 12 mission (1, 2). Seismic energy from the impact was recorded by the seismometers deployed on the lunar surface by the Apollo 12 astronauts as part of the emplaced science station called ALSEP (Apollo Lunar Surface Experiments Package). The seismic experiment is described by Latham *et al.* (3). The impact experiments have emerged as an extremely powerful tool in the seismic exploration of the moon. Their value is enhanced by the fact that relatively few seismic events of natural origin have been detected on the lunar surface. Thus, the seismic experiment will depend heavily on artificial sources, such as high-energy impacts, to determine the internal structure of the moon. It is expected that the National Aeronautics and Space Administration will include impacts of both the LM and the spent S-IVB stage of the Apollo booster on all future Apollo missions in which seismometers are included as part of the payload. Pertinent characteristics of the LM and S-IVB vehicles are given in Table 1. The purpose of this report is to aid in the interpretation of the lunar impact signals by presenting seismic data recorded from missile impacts at White Sands Missile Range.

Seismic signals from a total of five missile impacts were recorded between early 1968 and late 1969 at White Sands Missile Range, New Mexico. Signals were recorded by small geophone sensors and field recording equipment similar to the equipment used in oil exploration. The experi-

mental system has been described in detail by McDonald (4). The distances between the impact points and the various geophones are listed in Table 2. The geophones were laid out in a linear array for impact 5 and in triangular arrays for the remaining impacts. Good recordings were obtained on only one sensor in each of the first four impacts and on four sensors for impact 5. The kinetic energies of the impacts and the approximate weights

Table 1. Expended LM ascent stage and S-IVB impact parameters. Predictions for the S-IVB included allowances for angle of impact and gravitational acceleration (9, 11). Surface geometry has been ignored. For the LM, the estimates are very approximate and may be in error owing to lack of data for such low angles of impact. Data furnished by M. A. Persechino of the U.S. Naval Research Laboratory on the impact of 3.2-mm glass and aluminum spheres with phenolic nylon (density, 1.2 g/cm³) at 6.6 to 8.2 km/sec show that volumes of craters produced at angles of impact near 4° are 1/200 of craters for normal impacts and that crater volumes are near 1/12 of the projectile volume or 1/25 of the projectile mass. Thus, the volume of the crater produced by the LM may be near 10⁶ to 10⁷ cm³. Such a crater might be 0.10 m deep and several meters across.

Parameter	LM	S-IVB
Mass (kg)	2.57×10^8	1.39×10^4
Impact velocity (km/sec)	1.68	2.55
Kinetic energy of impact (ergs)	3.62×10^{16}	4.52×10^{17}
Equivalent energy (1 lb of TNT)	1.91×10^8	2.37×10^4
Angle of impact from horizontal	3.7°	74°
Predicted crater size		
Depth (m)	0.3 ± 0.2	14 ± 4
Diameter (m)	4 ± 2	57 ± 17

of TNT that would give equal energy release are listed for each impact in Table 2.

A typical seismic record obtained from a missile impact is shown in Fig. 1. Three types of signals are prominent on the records: (i) the initial arrival, which travels through the ground as a compressional wave (*P* wave); (ii) an emergent train of waves with particle motion confined to the near surface (Rayleigh waves); and (iii) a surface wave that travels at speeds near the speed of sound in air (air-coupled Rayleigh wave). The air-coupled Rayleigh wave is an additional train introduced by coupling of Rayleigh waves to atmospheric compressional waves (5). In the absence of an atmosphere, as on the moon, the air-coupled Rayleigh wave cannot propagate. Thus, we will not consider this phase further in the present report.

A fourth phase observed on some of the records from impacts 1, 2, 3, and 4 appears to correspond to the arrival of the direct pressure pulse that is heard as a loud boom by observers in the area of the impact. This impulse is marked *A* on the record shown in Fig. 1. The apparent velocity of this pulse is equal to the speed of sound in air, and it appears to originate at the impact point and not in the upper atmosphere at reentry. This pressure pulse, which radiates spherically from the impact point with the speed of sound in air, couples into Rayleigh waves. Since the seismic sensors are not pressure sensitive, the signal *A* is presumably produced by interaction between the pressure pulse and the sensor cables or local irregularities in the surface.

The observed *P* wave velocities range from 1.49 to 1.65 km/sec; Rayleigh wave velocities range from 0.49 to 0.57 km/sec; and the air-coupled Rayleigh wave has an apparent velocity of 0.339 km/sec.

The amplitudes (*a*) of the *P* waves were measured (see Fig. 2). For surface waves, the maximum peak-to-peak amplitudes were measured (see Table 2).

P wave and Rayleigh wave amplitudes from the missile impacts are plotted in Fig. 2 with curves given by Kovach (6) that represent a summary of seismic wave amplitudes from explosions. The left branch of the Kovach curves represents data from untamped surface explosions; the right branch corresponds to buried explosions. For a given impact, the scaled range is obtained by dividing the impact-detector

separation (in feet) by the cube root of the weight of TNT (in pounds), which would give energy release equal to the kinetic energy of the impact (1 ft = 30.48 cm; 1 lb = 453.59 g). Our rationale for comparing these explosion data is that, in many respects, impacts are similar in their effects to shallow explosions (7). Therefore, we assume that the seismic energy release from an impact cannot be greatly different from that of shallow explosions. Hence, the line that is fit through the impact data must have approximately the same slope as the line through the explosion data. [For the derivation of scaling laws applied here to describe explosion phenomena, see (8) and (9).

Seismic amplitude data from a series of five shallow explosions detonated as part of this study are also plotted in Fig. 2. From Fig. 2, it can be seen that impacts are more efficient than untamped surface explosions in generating *P* waves, but they are less efficient than buried explosions. This result is consistent with our expectations. For chemical explosions, a greater fraction of the total available energy would be used to heat the surrounding medium than would be the case for low-velocity impacts. For deeper explosions, however, this effect is outweighed by the efficiency gained through greater confinement of the released energy to the solid medium.

With the data of Fig. 2, we can estimate, for example, the distance from the point of impact of the LM or S-IVB to the point at which a *P* wave amplitude of 10 nm would be recorded. Referring to Fig. 2, the scaled range for a *P* wave amplitude of 10 nm is 1.9×10^3 ft/lb^{1/3}. The energy equivalent of the LM impact is 1910 lb of TNT. Thus, assuming negligible effects due to differences in angle of impact, the *P* wave amplitude produced by the LM impact would be 10 nm at a distance of 2.4×10^4 ft, or 7.2 km, from the point of impact. Similarly, the S-IVB impact would produce a *P* wave amplitude of 10 nm at a distance of 5.5×10^4 ft, or 16.8 km, from the point of impact. Implicit in these estimates are the assumptions (i) that the effective coupling of impact energy will be the same on the moon as for the missile impacts recorded in this study and (ii) that the transmissibility of the lunar material is the same as that of the material at the test range. The first assumption may certainly not be true for the very shallow angle of the Apollo 12 LM impact (3.7° from the hori-

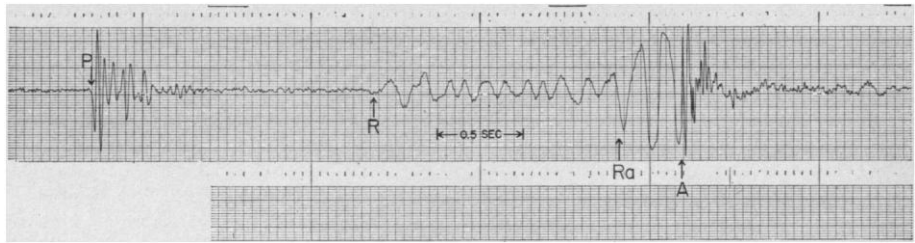


Fig. 1. Typical record of seismic signal from a missile impact. *P* = *P* wave; *R* = Rayleigh wave; *Ra* = air-coupled Rayleigh wave; *A* is assumed to be the direct pressure pulse arrival.

Table 2. Summary of impact data.

Impact No.	Impact-sensor separation (km)	Kinetic energy (ergs)	Equivalent weight* TNT (lb)	<i>P</i> wave		Rayleigh wave		Scaled range (ft/lb ^{1/3})
				Amplitude (μm)	Frequency (hz)	Peak-to-peak amplitude (μm)	Frequency (hz)	
1	0.423	1.35×10^{15}	71.1	0.46	20	1.9	10	357
2	0.402	1.45	76.3	0.35	23	2.1	10	332
3	1.16	1.52	80.0	0.30	21	1.7	6.7	942
4	1.54	1.51	79.5	0.35	24	0.77	5.3	1253
5	0.622	2.09×10^{14}	11.0	0.036	40	1.3	44	983
5	0.764	2.09	11.0	0.016	40	1.0	39	1197
5	1.00	2.09	11.0	0.017	40	0.78	23	1579
5	1.19	2.09	11.0	0.011	38	clip		2735

* Energy release of approximately 1.9×10^{13} ergs per pound of TNT is assumed (12).

zontal), but we take this estimate as a starting point. As to the second assumption, attenuation of seismic waves is apparently much lower for the outer regions of the moon than is typically observed for crustal regions on earth, a point discussed in greater detail below.

The relative efficiencies of shallow explosions and impacts as sources of seismic energy were determined by comparing the signals received from impact 5 with the signals recorded from a series of explosions detonated near the impact crater. Both the size and depth of burial of the explosive material were varied. The array of detectors and amplifier gains were the same in all cases. The results of this experiment are given in Table 3. The total mass displaced by the impact and by each of the five explosions, the scaled depth of burial of the charge, and the scaled range to each detector are also listed.

From these data we can determine the depth of burial of TNT with energy release equal to that of the kinetic energy of the impact that produces a crater of the same size as does the impact. The kinetic energy of impact 5 is equal to the energy release of approximately 11 lb of TNT. Moore has pointed out that the crater size expected from a given impact is a function of the angle of impact (10). The crater

size decreases as the angle between the impact trajectory and a line normal to the surface increases; however, this correction would be small in the present case. Plotting displaced mass versus depth of burial for the 10-lb shots, we find that the scaled depth (λ) for an explosion that would produce the impact crater is about $\lambda = 0.38$, where

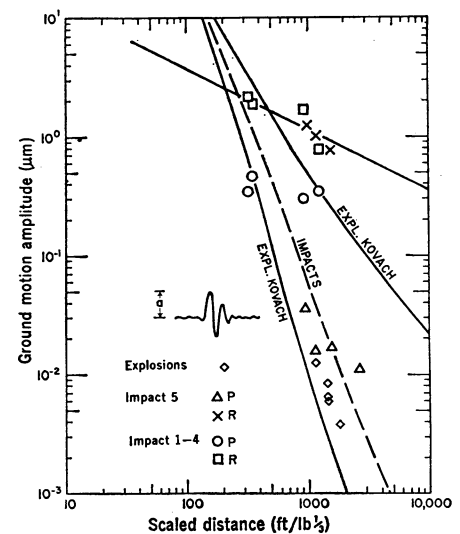


Fig. 2. Plot of *P* wave amplitudes (*a*) versus scaled range for impacts and explosions, and Rayleigh wave amplitudes (maximum peak to peak) versus scaled range for impacts. Points marked "explosions" are measured from data obtained in this study. Lines labeled "explosions" are taken from Kovach (6).

Table 3. Explosion versus impact data.

Event	Charge weight (lb)	Depth of burial* (inches)	P wave amplitude† (nm)	Mass displaced (g)	Scaled range‡ (ft/lb ^{1/3})	Scaled depth‡ (ft/lb ^{1/3})
Impact	11 (2 × 10 ¹⁴ ergs)	Surface	17	1.57 × 10 ⁶	1575	
Shot 1	5	10	3.8	0.85	1828	0.47
Shot 2	10	6.5	6.0	1.26	1453	0.24
Shot 3	10	13	6.5	1.94	1453	0.48
Shot 4	10	26	8.4	4.17	1453	0.95
Shot 5	20	16	12.5	4.30	1153	0.47

* Depth to center of charge. † Frequency is 25 to 29 hz for all events. Data are taken from a sensor located at a distance of 1.0 km. ‡ Energy equivalence for the explosive material is taken as 1.77 × 10¹³ ergs per pound (from information supplied by the manufacturer).



Fig. 3. Seismic signal received on the lunar long-period vertical component seismometer from the Apollo 12 LM impact.

the scaled depth is defined as the depth of the charge in feet divided by the cube root of the charge weight in pounds. Comparison between the amplitudes of the seismic signals produced by the impact and the amplitudes produced by the explosions at this scaled depth shows, however, that the fraction of available energy that goes into seismic waves is greater for the impact. Thus it is probable that a greater fraction of the total available energy is dissipated as heat for chemical explosions than for impacts at these velocities.

The LM impacted 75.9 km from the Apollo 12 lunar seismic station in the Sea of Storms. The signal recorded by the long-period vertical component seismometer is shown on a compressed time scale in Fig. 3. The character of this signal is strikingly different from that of the missile impact signals. As described by Latham *et al.* (1), the duration of the LM impact signal is extremely long (approximately 55 minutes) in comparison with the missile impact signals which, at a range of 75.9 km, would have lasted several minutes at most. Also, the LM impact wave train does not show the distinct seismic phases of Fig. 1. The LM impact wave train has a very emergent beginning, builds up slowly to a maximum over a period of approximately 6.8 minutes, and then gradually decreases in amplitude. The maximum signal amplitude is approximately 10 nm peak to peak with maximum spectral energy at approximately 1 hz. The amplitude of the beginning of the train is near the minimum de-

tectable signal of the system (0.3 nm). The velocity corresponding to the first detectable signal is approximately 3.2 km/sec. By measuring the rate of decay of the amplitude of the wave train, Latham *et al.* (2) have determined that the Q (quality factor) of the lunar material to depths of 10 to 20 km must be between 3000 and 5000. This value is in contrast with Q values of between 10 and 300 for most crustal materials on earth. Thus, the attenuation of seismic waves that propagate through the outer regions of the moon is extremely low compared with the attenuation observed for propagation through the crust of the earth. This observation may, of course, apply to the mare region in which the LM signal was recorded. The Q value at the White Sands test area for impact 5 was approximately 90, as determined from the decay of signal amplitude with distance.

As one hypothesis to explain the unexpected character of the LM impact signal, Latham *et al.* suggest that the moon not only has a high Q but is also very heterogeneous, at least to depths of 10 to 20 km (1). The nature of this heterogeneity, if indeed this interpretation of the data is correct, has important implications relative to the origin and evolution of the moon. The intense scattering of seismic waves that would occur through a highly heterogeneous material would tend to increase the duration of the wave train and to suppress the appearance of distinct phases. If this is so, the missile impact results would not be expected to apply, except possibly to the begin-

ning of the train where the effects of scattering would be least important.

From the data of Fig. 1, the predicted P wave amplitude for the LM impact is approximately 0.1 nm. This value should be increased by a factor of approximately 3 to account for the high Q inferred for the lunar material. Thus, the predicted value is 0.3 nm, which is in approximate agreement with the observed signal.

Latham *et al.* (2) obtain a value of between 0.0001 and 0.001 for the percentage of LM kinetic energy converted to seismic energy at the source. We obtain between 0.001 and 0.005 percent for the missile impact signals. The nearness of these results is surprising in view of the fact that the LM impacted the lunar surface at an angle of only 3.7° from the horizontal and the missile impact trajectories were much more nearly normal to the surface. A greater influence of angle of impact on the coupling of seismic energy would be expected.

Thus, the missile impact data presented here, when adjusted for the extremely low attenuation of the lunar material, provide a useful guide for predicting the amplitudes of the initial seismic signals produced by impacts on the lunar surface.

The complete lack of similarity between the lunar impact signal and the signals from the missile impacts reported here supports the view that the structure of the moon in the vicinity of the Apollo 12 landing site is radically different from the typical crustal structure of the earth.

For the impact of the S-IVB in April 1970, our results indicate that the P wave should be nearly detectable (amplitude of 0.3 nm) at a range of approximately 200 km.

It should be noted that these results cannot be applied directly to the problem of meteoroid impact dynamics, where impact velocities are normally much higher than the missile velocities of this study. For such impacts, a smaller fraction of the total available kinetic energy would be expected to be converted into seismic energy than was observed for the missile impacts.

GARY V. LATHAM

WILLIAM G. McDONALD

Lamont-Doherty Geological
Observatory, Columbia University,
Palisades, New York 10964

HENRY J. MOORE

U.S. Geological Survey,
Menlo Park, California

References and Notes

1. G. V. Latham, M. Ewing, F. Press, G. Sutton, J. Dorman, Y. Nakamura, N. Toksoz, R. Wiggins, J. Derr, F. Duennebier, *Science* **167**, 455 (1970).
2. G. Latham, M. Ewing, F. Press, G. Sutton, J. Dorman, Y. Nakamura, N. Toksoz, R. Wiggins, R. Kovach, "Apollo 12 Mission Science Report" (NASA Special Report, in press).
3. G. Latham, M. Ewing, F. Press, G. Sutton, *Science* **165**, 241 (1969).
4. W. McDonald, *Lamont-Doherty Geol. Observ. Tech. Rep. CU-2-69* (1969).
5. M. Ewing, W. Jardetzky, F. Press, *Elastic Waves in Layered Media* (McGraw-Hill, New York, 1957), p. 236.
6. R. Kovach, in *Physics of the Moon*, S. F. Singer, Ed. (American Astronautical Society, Science and Technology Series, Tarzana, California, 1967), p. 189.
7. H. J. Moore, in *Astrogeological Studies, Part B: Crater Investigations, Annual Progress Report, 1 July 1965-1 July 1966* (U.S. Geological Survey Open-File Report, 1966), p. 79.
8. R. Cole, *Underwater Explosions* (Princeton Univ. Press, Princeton, N.J., 1948).
9. A. Chabai, *J. Geophys. Res.* **70**, 5075 (1965).
10. H. J. Moore, *Science* **159**, 333 (1968).
11. S. W. Johnson, J. A. Smith, E. G. Franklin, L. K. Moraski, D. J. Teal, *J. Geophys. Res.* **74**, 4838 (1969).
12. M. D. Nordyke and W. E. Wray, *ibid.* **69**, 675 (1964).
13. We thank Lynn Sykes, Bryan Isacks, Reuben Kachadoorian, and Jerry P. Eaton for critically reviewing the manuscript. Data for the Lunar Module impact conditions were furnished by John Gurley, Manned Spacecraft Center, Houston, Texas. Jonathan B. Haussler, Marshall Spaceflight Center, Huntsville, Alabama, furnished the data for the S-IVB. Supported by NASA contract NAS9-5957. Lamont-Doherty Geological Observatory contribution No. 1501.

28 January 1970

Petroleum Lumps on the Surface of the Sea

Abstract. *Lumps of crude oil residue floating on the sea surface have been observed widely. Samples were taken with surface-skimming nets in the Mediterranean Sea and eastern North Atlantic Ocean; their displacement volumes were as large as 0.5 milliliter per square meter. An isopod, Idotea metallica, appears to be associated with the lumps, and a barnacle, Lepas pectinata, grows upon them. Lumps were found in stomachs of Scomberesox saurus, a surface-feeding fish important in ocean food webs. Films on the lumps, presumably consisting mostly of bacteria, consumed oxygen at the rate of 4 cubic millimeters per hour per square centimeter of lump surface. Chemical analysis suggested that certain lumps had been at large for only a few weeks; data from barnacle size and growth rate suggested that other lumps were at least 2 months old.*

Although oil pollution of the sea, particularly pollution resulting from spills and blowouts, has recently received considerable attention (1), little has been said (2) about the tarlike lumps that occur widely on the sea surface. We first noticed these lumps about 5 years ago when we began sampling the neuston, the fauna of the upper few centimeters of the sea, with surface-skimming nets (3). Since then we have found these variously sized, black or brownish-black lumps in many places in the North Atlantic. The lumps are so abundant that they regularly foul the neuston nets, which have to be cleaned repeatedly with solvents. Peter David of the National Institute of Oceanography, Wormley, England, has observed lumps since 1954 in the Mediterranean Sea and in the Atlantic and Indian oceans (4).

During cruise 49 of the R.V. *Atlantis II* between Rhodes (10 May 1969) and Ponta Delgada, Azores (28 June), tarry lumps were present in at least 75 percent of the 734 neuston tows made; the substance was recorded as absent in only 16 percent, and for a few tows no remark about the presence or absence of the tar was made. The displacement volumes of 41 samples of

tar are shown in Fig. 1 (5). Estimates from the neuston tows indicated that the amount of tar on certain areas of sea surface was as high as 0.5 ml/m².

The lumps were irregular in shape, with the greatest dimension varying from 1 or 2 mm to about 10 cm. Black lumps were commoner than brownish-black ones. Hardness varied, although all lumps were easily deformed by a

touch of the finger. The hardness of the softer ones could not be measured with the penetrometer used (6); the harder ones gave values of 0.1 to 0.3 kg/cm² (unconfined compressive strength). Some of the lumps were very sticky, had a rough, uneven surface, and were relatively soft and black. Other lumps were firmer with a smoother, more even surface and were usually lighter (brownish-black); this type frequently had barnacles attached and appeared to be older than the first. A sample of this tar (from 34°00'N, 26°00'E on 13 May) was soluble in chloroform and behaved in chromatography (7) as a typical crude oil.

The low-boiling fraction of crude oil, which contains the most immediately toxic substances (8), was retained in the lumps. It is evident that the formation of the petroleum into lumps tends to conserve these poisons. The presence of volatile components (7) suggests that this sample of tar had been at large for no more than a few weeks. One sample of tar collected on 18 May about 160 km off the coast of Libya contained bits of grass and leaves; it had probably been washed ashore and then out to sea again.

Several organisms were found on or were associated with the lumps. *Idotea metallica*, a pelagic isopod which ranged from 10 to 25 mm in length and varied from light gray to black in color, was collected in large numbers in the neuston nets and was frequently found clinging to lumps when a collection was dumped into the sorting tray. These isopods were also dipped from the sea surface together with the lumps.

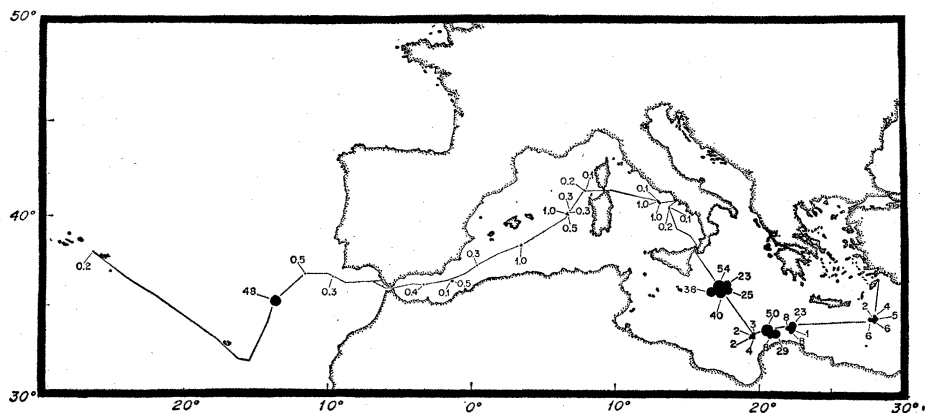


Fig. 1. Chart showing the distribution of petroleum lumps along a track in the Mediterranean Sea and the eastern North Atlantic. The area of the dots is proportional to the volume of the lumps collected; the numbers are the volumes in milliliters per square meter multiplied by 100. Collections were made nightly all along the track. Although some collections, particularly some west of Gibraltar, had too little tar to measure, almost all collections had at least a trace.